

Orbital Selectivity in Hund's metals: The Iron Chalcogenides

N. Lanatà,¹ H. U. R. Strand,² G. Giovannetti,³ B. Hellsing,² L. de' Medici,⁴ and M. Capone³

¹*Department of Physics and Astronomy, Rutgers University, Piscataway, New Jersey 08856-8019, USA*

²*Department of Physics, University of Gothenburg, SE-41296 Gothenburg, Sweden*

³*CNR-IOM Democritos National Simulation Center and Scuola Internazionale Superiore di Studi Avanzati (SISSA), Via Bonomea 265, 34136 Trieste, Italy*

⁴*Laboratoire de Physique des Solides, UMR8502 CNRS-Université Paris-Sud, Orsay, France*

(Dated: November 5, 2018)

We show that electron correlations lead to a bad metallic state in chalcogenides FeSe and FeTe despite the intermediate value of the Hubbard repulsion U and Hund's rule coupling J . The evolution of the quasi particle weight Z as a function of the interaction terms reveals a clear crossover at $U \simeq 2.5$ eV. In the weak coupling limit Z decreases for all correlated d orbitals as a function of U and beyond the crossover coupling they become weakly dependent on U while strongly depend on J . A marked orbital dependence of the Z 's emerges even if in general the orbital-selective Mott transition only occurs for relatively large values of U . This two-stage reduction of the quasi particle coherence due to the combined effect of Hubbard U and the Hund's J , suggests that the iron-based superconductors can be referred to as Hund's correlated metals.

PACS numbers: 71.30.+h, 71.10.Fd, 71.27.+a

The role of electron correlations in the iron-based superconductors is still a debated issue, naturally intertwined with the search for the origin of high critical temperatures. We present results that improve the qualitative understanding of how electron correlation influences fundamental electron properties of these compounds, such as the metallicity, which in turn might be important also for the understanding of the pairing mechanism. We choose two candidates of the chalcogenides, FeSe and FeTe and employ *first principles* electron structure calculations combined with advanced many-body methods taking into account the local electron correlation. The chalcogenides have in contrast to the pnictides a simpler atomic structure, thus easier to synthesize and also to study theoretically. In addition they are non toxic in contrast to the pnictides containing arsenic.

In previously known superconductors we can identify either weakly correlated materials, like elemental superconductors or binary alloys, including MgB₂, or highly-correlated compound like the copper oxides and heavy fermion materials. In the first set of compounds superconductivity is explained within the Bardeen-Cooper-Schrieffer framework and its extensions, and it occurs as a pairing instability of a normal metal. In the second set it is widely believed that correlations revolutionize the electronic properties and that both the metallic state and the pairing mechanism deviate from standard paradigms.

The iron-based pnictides and chalcogenides superconductors do not fit this simple classification. The common labeling "intermediate correlation", referring to properties such as Fermi surface topology or absence of Hubbard bands [1], suggests modest effects of correlations. Conversely, the metallic state appears much less coherent than what these observations imply [2, 3]. A magnetic counterpart of this dualism is the localized an itinerant

nature of the spin-density-wave state of the parent compound.

The characteristic property of the band structure is that several of the five d -bands cross the Fermi level. The multi-orbital nature leads to several exotic electronic properties such as orbital-selectivity [4–9] and also to the conclusion that the inter-orbital exchange or Hund's coupling plays a key role [10, 11].

The role of the Hund's coupling has indeed been recognized in the early stages of the field in a Dynamical Mean-Field Theory (DMFT) study by Haule and Kotliar [10], who coined the definition of Hund's metals by the observation that the quasi particle effective mass and the response functions are much more sensitive to the Hund's coupling J than to the Hubbard U interaction.

For a Hund's metal the spectral weight is not transferred to the high-energy Hubbard bands, but rather spreads over a scale controlled by J . Other DMFT studies have highlighted the anomalies of the metallic state, showing its incoherent nature [12, 13] and its relation with a spin-freezing crossover [14]. In Ref. [15] the dual nature of the magnetic correlation is shown to induce a remarkable difference between a large instantaneous magnetic moment and smaller long-time magnetic correlations, similar to the spin-freezing scenario proposed in Ref. [16] for a three-orbital model.

It has recently been shown that J can have a two-fold effect on a multiorbital system with an integer filling different from one electron per orbital [17], a situation which is realized in the parent compounds of iron superconductors, in which six electrons populate the five d orbitals. In this configuration J reduces the quasi particle coherence temperature (or coherence energy scale), while it increases the critical U for the Mott transition.

As a consequence, a two-stage reduction of the elec-

tronic coherence scale (measured by the quasi particle weight Z) occurs as a function of U . Indeed, if we choose a sizable value of J and follow the evolution of the metallic properties, we first have a rapid decrease of the effective Fermi-liquid coherence scale, which leads to a bad metal already for intermediate correlations strengths, while the Mott transition occurs only at much larger U . This opens a window of U in which Z is essentially flat, which has been dubbed after the roman god Janus in view of the double-faced effect of the Hund's coupling [17].

In this work we explore the combined role of U and J in the iron-based chalcogenides FeSe and FeTe by means of the Gutzwiller approximation (GA). The GA is a simplified treatment of electron correlations which systematically selects the energetically favorable electronic configurations out of an uncorrelated wave function. The method provides a reasonable description of the Mott transition from the metallic side [18] and allows for a numerically cheap investigation of a wide range of model parameters.

We employ the GA numerical scheme developed in Ref. [19–21], which is a generalization of earlier formulations of the GA method [22–25] and which enables taking into account the full rotationally invariant Hund's terms, including the so-called spin-flip and pair-hopping, that are often hard to treat with approximate analytical methods and even with numerical methods. Since the formation of a Hund's metal is actually associated with a differentiation between the different atomic multiplets, we expect that the GA will perform even better than for standard Mott transitions.

Based on electronic structure calculations of FeSe and FeTe combined with the GA we show that the electronic configuration of the parent compounds of iron-based superconductors form an ideal system with a two-stage reduction of electronic coherence. Furthermore, the bad metal arising from the interplay of U and J displays, as expected, an orbital-selective coherence with t_{2g} orbitals significantly more correlated than e_g .

The material-specific band structure is determined using Density Functional Theory with the Generalized Gradient Approximation for the exchange-correlation potential according to the Perdew-Burke-Ernzerhof recipe as implemented in Quantum Espresso [26]. Then we apply Wannier90 [27] to compute the maximally localized Wannier orbitals, and we include the interaction terms of the form

$$H = U \sum_{i,m} n_{im\uparrow} n_{im\downarrow} + (U' - \frac{J}{2}) \sum_{i,m>m'} n_{im} n_{im'} \quad (1)$$

$$- J \sum_{i,m>m'} [2\mathbf{S}_{im} \cdot \mathbf{S}_{im'} + (d_{im\uparrow}^\dagger d_{im\downarrow}^\dagger d_{im'\uparrow} d_{im'\downarrow} + \text{H.c.})].$$

Here $d_{i,m\sigma}$ is the destruction operator of an electron of spin σ at site i in orbital m , and $n_{im\sigma} \equiv d_{im\sigma}^\dagger d_{im\sigma}$, $n_{im} \equiv \sum_{\sigma} d_{im\sigma}^\dagger d_{im\sigma}$, \mathbf{S}_{im} is the spin operator for orbital

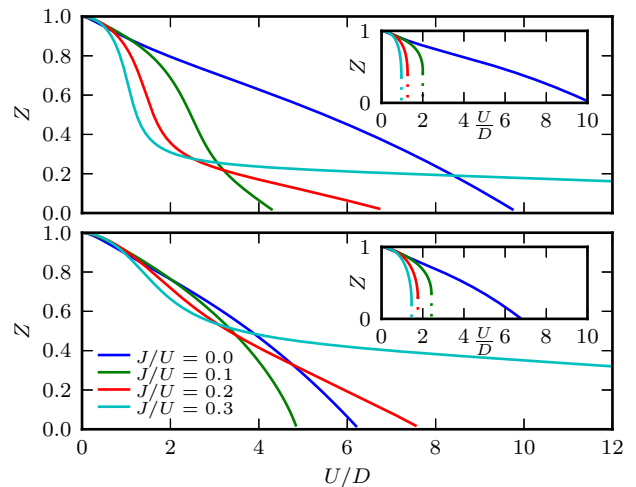


FIG. 1: Quasiparticle weight in a N_{orb} -fold degenerate Hubbard model with average population of $N_{\text{orb}}+1$ electrons, as a function of U/D for various Hund's coupling J/U , where D is the half-bandwidth. Upper panel: $N_{\text{orb}}=5$, Lower panel $N_{\text{orb}}=3$. The panels show data for $N=N_{\text{orb}}+1$ electrons, the insets for $N=N_{\text{orb}}$.

m at site i . U and $U' = U - 2J$ are intra- and inter-orbital repulsions and J is the Hund's coupling. The values of U and J are not directly accessible from experiments and even if reliable theoretical estimates are obtained with constrained-RPA, there are still some discrepancies between different calculations. In the light of the extreme sensitivity on the value of the parameter J , it is particularly useful to apply a method such as the present GA which allows for a continuous sweep of many parameter values.

As mentioned above, one of the distinctive features of the iron-based superconductors is that all five d -orbitals appear to contribute to the band structure around the Fermi level. As a first step we consider a system with five degenerate d bands, and show that the configuration with six electrons per atom, characteristic of the parent compounds, is a clear cut case of a ‘‘Janus’’ scenario, characterized by a two-stage reduction of the quasi particle weight.

In Refs. [11, 17] it is clearly shown that the two-stage reduction of the electronic coherence scale is a consequence of a contrasting effect of J on the metallic character of the electrons. In the weak-coupling limit J favors the formation of a large local magnetic moment, which leads to a faster decay of the electronic coherence scale Z , while in the strong-coupling the Mott transition is pushed to larger U . This effect is particularly strong when the number of electrons per atom differs by one unit from the number of orbitals $N = N_{\text{orb}} \pm 1$, and it is expected to be emphasized increasing the number of orbitals as the weak-coupling coherence temperature scales exponentially with N_{orb} .

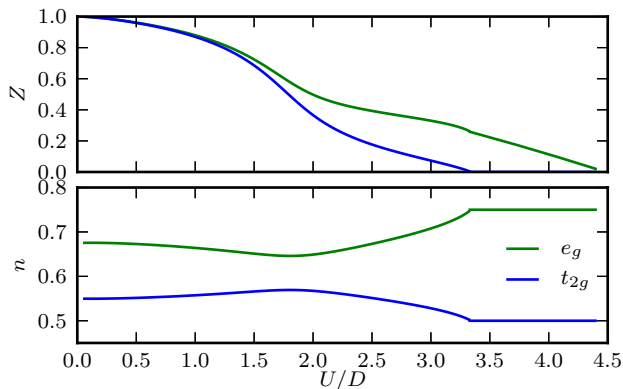


FIG. 2: Upper panel: quasiparticle weight in a Hubbard model with 6 electrons in 5 bands with semi-circular densities with half-bandwidth D split by a cubic crystal-field in two manifolds of degeneracy 3 (t_{2g} symmetry) and 2 (e_g symmetry). Lower panel: populations of the two manifolds.

In Fig. 1 we compare the GA results for the two cases of $N = N_{\text{orb}} \pm 1$ when $N_{\text{orb}} = 5$ and $N_{\text{orb}} = 3$. We clearly see that the former case has a much clearer separation between a regime in which Z rapidly decreases as a function of U and a large bad metal region in which Z is essentially constant prior to the Mott insulator transition. In the inset we show the case of half-filling, $N = N_{\text{orb}}$, where no dual nature is observed.

Once established that the electron count of the parent compounds of the iron-based superconductors gives rise to a strongly two-faced correlation physics, we move towards the realistic situation in order to identify how the material-specific properties influence this picture. As an intermediate step, we lift the degeneracy with a cubic crystal-field which is present in iron pnictides and chalcogenides. An energy splitting Δ is introduced between the three t_{2g} and the two e_g orbitals. In Fig. 2 we show the results for $\Delta/D = 0.2$. We observe that, while the weak-coupling region gives an essentially orbital-independent Z , as soon as we enter in the strongly correlated region, the low-lying states become more correlated than the higher-lying. In other words, the crystal-field triggers a strongly orbital-selective renormalization in the bad metal state.

We finally perform the realistic DFT+GA calculation for iron chalcogenides. In panel (a) of Fig. 3 we show the evolution of the quasi particle weight for the different orbitals as a function of U , keeping the ratio J/U fixed to 0.224. This ratio is chosen according to the estimates presented in Ref. [28] for FeSe. The picture remains similar to the idealized systems. For small values of U the Z 's for the different orbitals are similar and they appreciably decrease as a function of U before $U \simeq 2.5$ eV, where the system enters the novel regime in which the Z 's are small and almost constant as a function of U . However, an orbital dependence also appears clearly. In addition

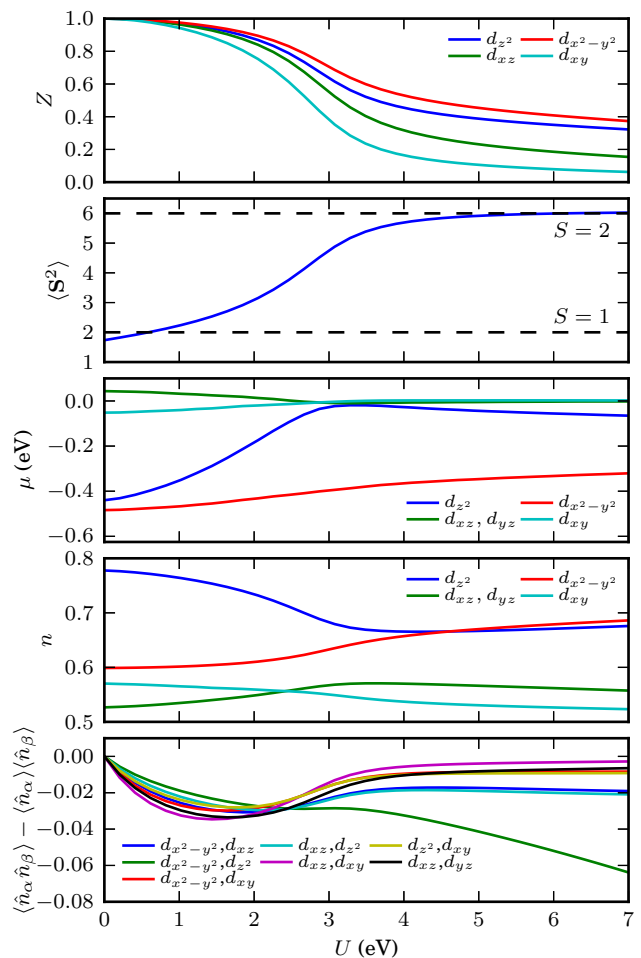


FIG. 3: Results for FeSe (DFT+GA with $J/U = 0.224$) as a function of U . From the top; panel (a), the quasi particle weights for the different orbitals, in panel (b) the expectation value of S^2 , in panel (c) the renormalized crystal-field splittings, in panel (d) the population of each orbital, in panel (e) the inter-orbital density correlations.

to the differentiation of the t_{2g} and e_g orbitals, we find that the d_{xy} orbital is the most correlated and the $d_{x^2-y^2}$ is more localized than the $d_{3z^2-r^2}$. The crossover, which roughly separates a weakly-correlated phase from a bad metallic phase, takes place at a value of U smaller than the bandwidth $2D$ (~ 4 eV), and much smaller than the multiband Mott transition, which would take place at a U of the order of 5 times the width of each band [29].

It is easy to see that in the atomic limit the ground state changes from low-spin ($S = 1$) to high-spin ($S = 2$) when J becomes larger than the crystal-field splittings (~ 0.6 eV for FeSe). In the metallic phase this evolution yields a crossover to a $S = 2$ state (Panel (b)) which leads to the rapid reduction of Z [11].

This crossover leads to a dramatic lowering of the coherence temperature, and opens a wide bad-metal region due to the increase of U_c induced by the effect

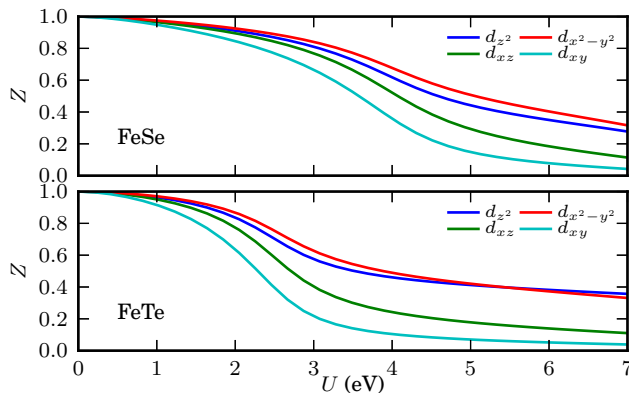


FIG. 4: Results for FeSe and smaller $J/U = 0.15$ (top panel) and for FeTe (bottom panel)

of J on the high-spin Mott gap. This behavior is observed even more pronounced in studies of LaFeAsO [30] and the intercalated chalcogenides [31]. It contributes in a substantial manner to the sharp onset of the Hund’s metal [10]/spin-frozen [14]/incoherent [12, 13] phase observed in all DMFT studies.

This effect is also reflected in the renormalized orbital energies (panel (c) of Fig. 3), with four of the five orbitals being brought close to one another and also near the Fermi level by the interactions. This favors a more even population of the orbitals that gains in exchange energy, and favors the high-spin configurations over the low-spin ones. The evolution of the population of the different orbitals is shown in panel (d) of Fig. 3. The t_{2g} orbitals have populations closer to half-filling already at the DFT level, while the e_g bands are more occupied. Increasing the interaction the d_{xy} level, which has the smaller Z , becomes less occupied than d_{xz} and d_{yz} due to the stronger effect of correlations. Analogously, the large difference between the non-interacting densities of the two e_g bands is washed out by correlations, which favor a more democratic occupation with high spin. The same low to high spin transition within the metallic phase occurs for any sizable value of J and it is indeed present already in the model with a simple t_{2g} - e_g splitting as clear from the non-monotonic population behavior shown in the lower panel of Fig. 2.

In Panel (e) of Fig. 3 we show the inter orbital density correlation functions, which are clearly suppressed in the correlated regime. This suppression, driven by J , has been put forth [4, 29] as the driving mechanism behind the orbital selectivity. Indeed J acts as an “orbital decoupler” (“band decoupler” [29], for weak orbital hybridization) suppressing inter-orbital charge fluctuations, and rendering the charge dynamics of each orbital virtually independent. For a smaller value of J/U , 0.15, the picture does not change. The position of the crossover is only weakly affected, while the values of the Z ’s in the

bad metallic region after the crossover depend strongly on J . The behavior observed confirms previous findings of a Z which depends strongly on J and weakly on U in the physically relevant region of $U \sim 4$ eV and $J \sim 0.5 - 1$ eV. At the same time our results clearly underline that such “Hund’s metal” requires a critical value of the Hubbard repulsion, albeit much smaller than one might expect on the basis of the value of the bandwidth. The picture is clearly consistent with that drawn in Ref. [17]. Finally, we show the quasi particle weights for FeTe using the same value of the interaction coefficients. The main difference is a sharper separation between t_{2g} and e_g orbitals, and a larger renormalization for the e_g orbitals.

In summary, we have calculated the correlation strength induced by many-body correlations on the ab-initio electronic structure of the iron chalcogenides FeSe and FeTe. We find, in agreement with previous analogous studies on LaFeAsO [30] and $K_{1-x}Fe_{2-y}Se_2$ [31], that Hund’s coupling has a strong influence on the electronic properties of the paramagnetic phase, inducing a two-stage quasi particle renormalization. A first regime at weak coupling sees a moderate correlation affecting all orbitals comparably. After a quick decrease around $U \simeq 2.5$ eV, a value much smaller than the overall bandwidth, a strongly correlated regime is entered, heavily differentiated among the orbitals (with t_{2g} orbitals sensibly more correlated), in which the quasi particle weights are almost independent of U . The Mott transition occurs at much higher (~ 5 times the bandwidth) interaction strengths. Comparison with idealized models shows that the two-staged reduction of the quasi particle weights is due to the filling of 6 electrons in 5 bands, thus placing the system in the “Janus” regime induced by Hund’s coupling [17], and that, by introducing a crystal-field t_{2g} - e_g splitting, orbital differentiation happens once entered the Janus regime, where the orbitals closest to half-filling are more correlated [29].

We acknowledge useful discussions with L. Bascones. M.C. and G.G. acknowledge financial support of FP7/ERC through Starting Independent Research Grant “SUPERBAD” (Grant Agreement n. 240524). H.U.R.S acknowledges funding from the Mathematics Physics Platform (MP2) at the University of Gothenburg. L.d.M. acknowledges funding from Agence Nationale de la Recherche (project ANR-09-RPDOC-019-01). The calculations were partly performed on resources provided by the Swedish National Infrastructure for Computing (SNIC) at Chalmers Centre for Computational Science and Engineering (C3SE) (project 001-10-37).

-
- [1] W. L. Yang et al., Phys. Rev. B **80**, 014508 (2009).
 - [2] G. R. Stewart, Rev. Mod. Phys. **83**, 1589 (2011).

- [3] D. C. Johnston, *Adv. Phys.* **59**, 803 (2010).
- [4] L. de' Medici, S. R. Hassan, M. Capone, and X. Dai, *Phys. Rev. Lett.* **102**, 126401 (2009).
- [5] L. de' Medici, S. R. Hassan, and M. Capone, *J. Supercond. and N. Mag.* **22**, 535 (2009).
- [6] S. P. Kou, T. Li, and Z. Y. Weng, *Europhys. Lett.* **88**, 17010 (2009).
- [7] A. Hackl and M. Vojta, *New J. Phys.* **11**, 055064 (2009).
- [8] W.-G. Yin, C.-C. Lee, and W. Ku, *Phys. Rev. Lett.* **105**, 107004 (2010).
- [9] E. Bascones, B. Valenzuela, and M. Calderon (2012), arXiv:1208.1917.
- [10] K. Haule and G. Kotliar, *New J. of Phys.* **11**, 025021 (2009).
- [11] A. Georges, L. de' Medici, and J. Mravlje (2012), ArXiv:1207.3033v2.
- [12] H. Ishida and A. Liebsch, *Phys. Rev. B* **81**, 054513 (2010).
- [13] A. Liebsch and H. Ishida, *Phys. Rev. B* **82**, 155106 (2010).
- [14] P. Werner, M. Casula, T. Miyake, F. Aryasetiawan, A. J. Millis, and S. Biermann, *Nat. Phys.* **8**, 331 (2012).
- [15] P. Hansmann, R. Arita, A. Toschi, S. Sakai, G. Sangiovanni, and K. Held, *Phys. Rev. Lett.* **104**, 197002 (2010).
- [16] P. Werner, E. Gull, M. Troyer, and A. Millis, *Phys. Rev. Lett.* **101**, 166405 (2008).
- [17] L. de' Medici, J. Mravlje, and A. Georges, *Phys. Rev. Lett.* **107**, 256401 (2011).
- [18] W. F. Brinkman and T. M. Rice, *Phys. Rev. B* **2**, 4302 (1970).
- [19] N. Lanatà, H. U. R. Strand, X. Dai, and B. Hellsing, *Phys. Rev. B* **85**, 035133 (2012).
- [20] N. Lanatà, Y. Yao, and G. Kotliar, Unpublished (2012).
- [21] H. U. R. Strand, N. Lanatà, M. Granath, and B. Hellsing, Unpublished (2012).
- [22] M. Fabrizio, *Phys. Rev. B* **76**, 165110 (2007).
- [23] N. Lanatà, P. Barone, and M. Fabrizio, *Phys. Rev. B* **78**, 155127 (2008).
- [24] N. Lanatà, P. Barone, and M. Fabrizio, *Phys. Rev. B* **80**, 224524 (2009).
- [25] X. Deng, L. Wang, X. Dai, and Z. Fang, *Phys. Rev. B* **79**, 075114 (2009).
- [26] P. Giannozzi et al., *J. Phys. Cond. Matter* **21**, 395502 (2009).
- [27] A. A. Mostofi, J. R. Yates, Y.-S. Lee, I. Souza, D. Vanderbilt, and N. Marzari, *Comput. Phys. Commun.* **178**, 685 (2008).
- [28] M. Aichhorn, S. Biermann, T. Miyake, A. Georges, and M. Imada, *Phys. Rev. B* **82**, 064504 (2010).
- [29] L. de' Medici, *Phys. Rev. B* **83**, 205112 (2011).
- [30] R. Yu and Q. Si, *Phys. Rev. B* **86**, 085104 (2012).
- [31] R. Yu and Q. Si (2012), 1208.5547.